

The Distribution of Sn Between CaO–CuO_x–FeO_y–SiO₂ Slag and Copper Metal at 1300 °C



A. Van den Bulck, S. Turner, M. Guo, A. Malfliet and B. Blanpain

Abstract In Europe, 50% of the copper originates from recycling. High-Cu containing scraps are regularly rich in impurities like Fe, Ni, Sn and Pb. Many high-Cu containing scraps are fed directly into anode-furnace casting installations or furnaces with limited refining capability. The impurities levels of the anodes produced in these processes should however remain acceptable for further electro-refining. The distribution of Sn between copper and slag has been investigated for conditions relevant to copper converting. Unlike previous studies, this work focuses on the behavior of Sn relevant to fire refining conditions, which are essential for anode refineries. In this study, liquid Cu–1Sn and CuO_x–FeO_y–SiO₂ slag, with CaO additions, were equilibrated at 1300 °C in vacuum sealed SiO₂ ampoules. After metal–slag equilibration, the samples were quenched in water. The composition of the slag and Cu metal was investigated with Electron Probe X-ray Microanalysis. The distribution coefficients of Sn between slag and Cu metal were determined as a function of slag composition.

Keywords Anode copper · Sn distribution ratio · Slag
Electron probe micro-analysis

Introduction

In Europe, 50% of the copper originates from recycling [1]. These secondary copper streams regularly contain impurities like Fe, Ni, Sn and Pb in significant amounts. After fire refining of copper, these impurities remain in the anode copper, which leads to problems in electrorefining. During fire refining, a ‘Cu₂O’–‘Fe₂O₃’–SiO₂

A. Van den Bulck (✉) · M. Guo · A. Malfliet · B. Blanpain
Department of Materials Engineering, KU Leuven,
Kasteelpark Arenberg 44, bus 2450, B-3001 Leuven, Belgium
e-mail: amy.vandenbulck@kuleuven.be

S. Turner
Aurubis Belgium RD&I, Watertorenstraat 25, 2250 Olen, Belgium

© The Minerals, Metals & Materials Society 2018
B. Davis et al. (eds.), *Extraction 2018*, The Minerals, Metals & Materials Series,
https://doi.org/10.1007/978-3-319-95022-8_87

1083

slag is used. Hidayat et al. [2, 3] studied the liquidus surfaces of this system in equilibrium with metallic copper–iron alloy.

Five primary phase fields (ppf) bind the liquid region, i.e. cuprite (Cu_2O), delafossite (CuFeO_2), spinel (“ Fe_3O_4 ”), tridymite (SiO_2) and wustite (FeO). At 1300 °C, the liquid region is bound by cuprite, tridymite, and spinel. The p.p.f.’s relevant for fire refining conditions are tridymite and spinel. The authors [3] mentioned that when the oxygen partial pressure of the system decreases, the composition of the slag moves away from the Cu_2O corner and approaches the Fe_2O_3 – SiO_2 binary. Thus, based on the Cu_2O concentration of the slag, an estimation of the oxygen partial pressure can be made.

The distribution of Sn between copper and slag has been investigated for conditions relevant to copper converting [4–7]. Unlike the previous studies, this work focuses on the Sn distribution relevant to fire refining conditions, i.e. higher copper content in slag and presence of CaO, as CaO is a common component in fire refining slags. The Sn distribution coefficients were determined at 1300 °C for additions of 3, 5 and 10 wt% CaO in the tridymite ppf.

Experimental Technique and Procedure

High purity (>99.9%) powders were supplied by Sigma-Aldrich (CaO, Cu_2O , Fe, SiO_2), Alfa-Aesar (Fe_2O_3), and Atlantic Equipment engineer (Sn). The oxide powders and Fe were mixed with an agate mortar and pestle and then pelletized. Cu–1Sn alloy was made by heating the metal Sn powder and the copper metal (99.9995%, OFE, Aurubis N.V., Belgium) to 1200 °C in a vertical tube furnace in a closed vacuum sealed SiO_2 ampule. The alloy was turned to obtain alloy shavings. The samples were made by weighing 0.05 g of the oxide mixture and 0.06 g of alloy. The oxide-metal mixtures were put in SiO_2 ampules with an ID of 11 mm and a height of ± 8 mm, which were subsequently vacuum sealed. The ampoules were suspended from a kanthal wire (Sandvik Benelux B.V.) in a vertical tube furnace (impervious recrystallized alumina, 80-mm ID, GERO HTRV100-250/18) with MoSi_2 heating elements. The temperature was monitored by Pt/Pt–13%Rh thermocouple. As suggested by Ilyushechkin et al. [8], the samples were heated to 50 °C above the chosen equilibrium temperature (1300 °C) for 30 min, followed by equilibrating at the chosen equilibrium temperature, to ensure equilibrium between liquid and solid. The samples were quenched, after 12 h, in a bucket of water at room temperature with an immersed refractory brick in the bucket. The height of the water above the brick was approximately 2 cm, such that the ampule breaks upon hitting the brick and a faster quench is obtained. A schematic is shown in Fig. 1.

Electron Probe Microanalysis (EPMA) was used to determine the chemical composition of the slag phase, copper phase and the tridymite phase. The samples were prepared by embedding the material with EpoFix (Struers), followed by one day curing under vacuum. The samples are ground and polished using conventional

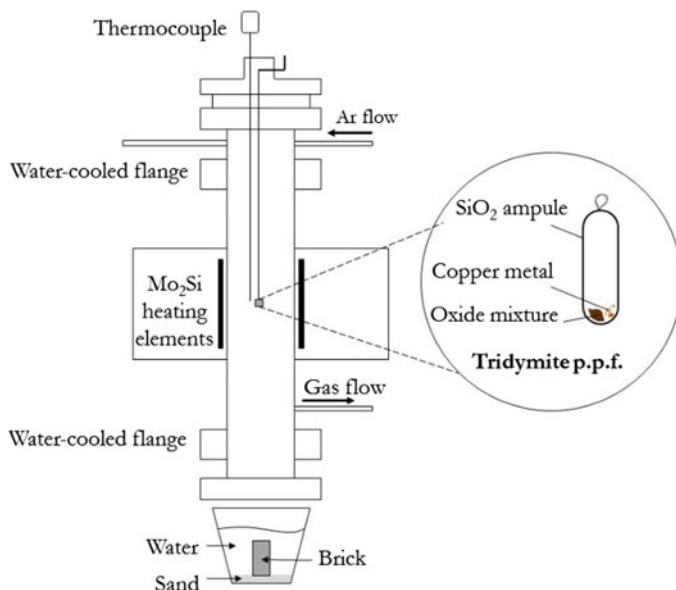


Fig. 1 Furnace set up with Mo₂Si heating elements and Ar flow. The sample is in direct contact with the SiO₂ ampule for the experiments performed in the tridymite p.p.f. The sample is dropped onto a refractory brick which was placed in a bucket of water

techniques, and then carbon coated approx. 20 nm high with a QT150TE carbon coater. A FEG-EPMA JEOL JXA-8530F was used to determine the chemical compositions of the phases. To calibrate the EPMA, Fe₂O₃, SiO₂, Sn, MgCaSiO₆ (SPI Supplies, USA), Cu₂O, Cu (Aurubis N.V., Belgium) and SnO₂ (Ibwenge, Congo) standards were used. The iron oxide, copper oxide and tin oxide concentrations were reported as Fe₂O₃, Cu₂O, and SnO₂, respectively.

Discussion of Microstructure

The purpose of quenching is to retain the phases that are present at the equilibrium temperature. However, samples are not always well quenched. Figure 2a shows the back-scattered electron (BSE) micrograph of a typical slag–metal–solid microstructure. Figure 2b shows a zoomed-in BSE micrograph. The images show a large copper droplet (Cu), a slag phase (S) and some tridymite crystals (T). In the slag, several submicron copper particles can be seen. Most likely, the copper precipitated from the slag during quenching. These issues have been mentioned by other authors as well [9, 10].

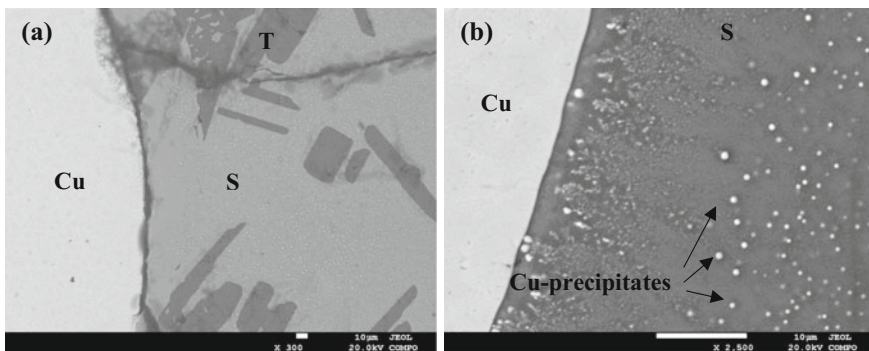


Fig. 2 **a** Back-scattered electron (BSE) micrograph showing copper (Cu), slag (S) and tridymite (T) crystals; **b** BSE micrograph of the Cu and slag. The presence of submicron copper precipitates is visible near the copper droplet

Selection of EPMA-Parameters

As mentioned before, some copper precipitated from the slag. Figure 3a shows the BSE micrograph and Fig. 3b shows the measured Cu_2O concentration in the slag using different acceleration voltages and fixed probe diameters. The average compositions for 20 and 15 kV are similar. However, the standard deviation decreased when using a defocused beam of 5 μm . This result is most likely due to the presence of submicron copper particles, which precipitated from the matrix upon quenching. Thus, local composition changes can be measured when using a small probe diameter. The use of a defocused beam was also applied by Fallah-Mehrjardi et al. [10].

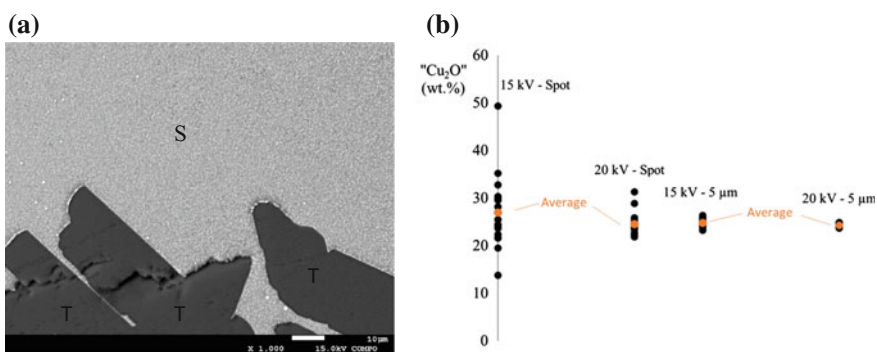


Fig. 3 **a** Back-scattered electron micrograph showing the copper precipitates in the slag (S) and the tridymite crystals (T); **b** copper oxide content in slag as function of acceleration voltage and EPMA probe diameter (i.e. focused beam (spot) and a defocused beam of 5 μm)

To determine the composition of the slag phases, the accelerating voltage and probe current were set to 20 kV and 50 nA, respectively and the standard Duncumb-Philibert ZAF corrections were applied. Eventually, a non-zero diameter probe of 20 μm was used for further investigations based on the level of heterogeneity of the other samples.

The Sn in the copper phase is expected to be far less than 1.0 wt% and measuring these low levels can be challenging. However, the EPMA is an adequate analytical technique to measure these low levels or trace elements [11].

The optimum conditions to improve the precision for trace element analysis are maximization of the net counting rate on the peak position (P/t) and the peak-to-background ratio (P/B). The two can be increased by increasing the beam current and the acceleration voltage, which increase the intensity of the characteristic X-rays. Long counting times (t) can be employed as well. However, the presence of beam current drift, specimen damage and increased interaction volume need to be taken into account [11, 12]. The high acceleration voltages and high electron beam currents are a practical approach for copper.

Figure 4a shows the limit of quantification (LOQ) as a function of probe current on a Aurubis foxrod reference sample (99.9995%, OFE, Aurubis N.V., Belgium) as a function of beam current. Figure 4b shows a wavelength scan of the influence of probe current around the Sn–L _{α} line in a copper phase. At higher probe currents, the (P/B) does not change significantly. However, the LOQ, i.e. the lower limit of the concentration that can be reported, decreases significantly. At 500 nA and 10 s on peak counting time, the LOQ is measured to be 0.045 wt%. Measured Sn concentrations below this level cannot be reported accurately.

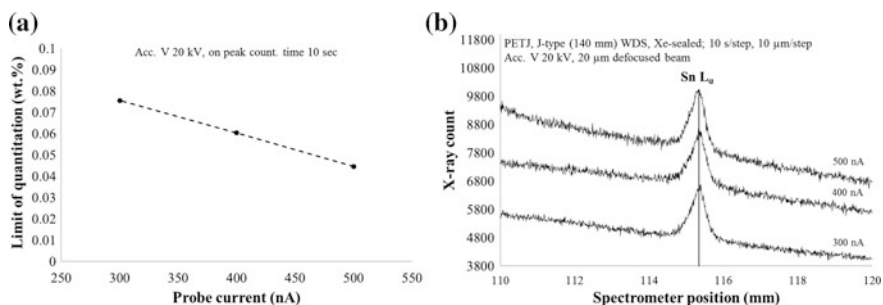


Fig. 4 **a** Limit of quantification for Sn (<1 ppm) in Aurubis foxrod reference sample (99.9995% Cu, OFE, Aurubis N.V., Belgium) as a function of beam current. The limit of quantification was calculated by the equation: $\text{LOQ} = 10 \times s$ where s is the standard deviation on a blank measurement. **b** WDS intensity scan of the Sn–L _{α} line (PETJ, Xe-sealed) in a copper droplet for various beam currents

The accelerating voltage and probe current for Sn in the copper phase were set to 20 kV and 500 nA, respectively and the standard Duncumb-Philibert ZAF corrections were applied. A non-zero diameter probe of 20 μm was used as well.

Discussion Homogeneity of Sample

As mentioned by several authors [3, 9, 10], a common practice to confirm thermodynamic equilibrium is to confirm the homogeneity of a chemical phase. Figure 5 shows the back-scattered electron images of copper phase and slag phase. Compositional measurements (wt%) were made in different regions of the slag phase (denoted by the numbers), as well as the copper phase (denoted by the letters). The measurements in the slag phase and the copper phase are shown in Tables 1 and 2, respectively.

In the different areas of the slag, the measurement results do not change significantly and the relative standard deviations are less than 3.0%. Similarly, for the copper droplets, the results do not vary significantly. However, for the measurements of Sn in the copper droplets, the standard deviations are higher than that for the slag measurements and can reach up to 26.8% for low concentrations of Sn. Therefore, to ensure accuracy, it is a necessity to have a significant amount of measurements.

As the measured compositions in different areas of the same sample are similar, it is assumed that chemical equilibrium was achieved within the samples after 12 h of equilibration time.

Fig. 5 Back-scattered electron micrograph showing copper droplets, slag and tridymite crystals. The numbers show different regions that were measured in the slag and the letters are different regions that were measured in the copper droplets

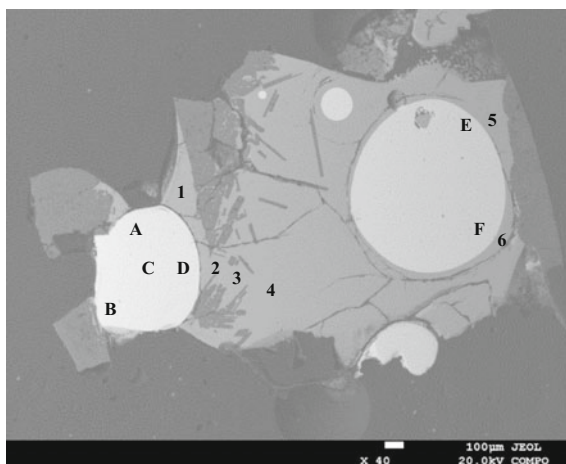


Table 1 Experimentally determined phase compositions (wt%) in different areas of the same CaO–CuO_x–FeO_y–SiO₂–SnO₂ slag in equilibrium with copper metal at 1300 °C. The results do not show any large deviations and it indicates that chemical equilibrium is achieved

		SiO ₂	“Cu ₂ O”	“Fe ₂ O ₃ ”	“SnO ₂ ”	CaO	Total
Area 1 (20 points)	Average (wt%)	35.7	20.8	38.2	1.57	4.15	100.4
	Standard deviation (wt%)	0.2	0.3	0.2	0.03	0.03	0.5
	Relative standard deviation of average (%)	0.4	1.5	0.4	2.0	0.6	0.5
Area 2 (11 points)	Average (wt%)	35.7	20.3	38.4	1.58	4.20	100.2
	Standard deviation (wt%)	0.2	0.2	0.2	0.06	0.01	0.3
	Relative standard deviation of average (%)	0.5	1.1	0.5	3.7	0.4	0.3
Area 3 (13 points)	Average (wt%)	35.7	20.5	38.5	1.56	4.18	100.5
	Standard deviation (wt%)	0.5	0.7	0.2	0.03	0.03	0.8
	Relative standard deviation of average (%)	1.3	3.6	0.6	1.7	0.7	0.8
Area 4 (10 points)	Average (wt%)	35.7	20.4	38.5	1.6	4.2	100.4
	Standard deviation (wt%)	0.3	0.6	0.2	0.04	0.03	0.6
	Relative standard deviation of average (%)	1.0	2.8	0.6	2.8	0.6	0.6
Area 5 (28 points)	Average (wt%)	36.1	20.5	38.7	1.53	4.17	101.1
	Standard deviation (wt%)	0.5	0.7	0.5	0.04	0.05	0.5
	Relative standard deviation of average (%)	1.4	3.6	1.4	2.5	1.1	0.5
Area 6 (20 points)	Average (wt%)	36.1	21.5	37.6	1.6	4.1	100.9
	Standard deviation (wt%)	0.2	0.5	0.5	0.04	0.01	0.4
	Relative standard deviation of average (%)	0.5	2.5	1.3	2.8	0.3	0.4

Distribution of Sn Between CuO_x–FeO_y–SiO₂–CaO Slag and Copper Metal

Yazawa [6] described the distribution ratio of a metal, M, between metal (m) and slag (s) as:

$$L_M^{s/m} = \frac{(\text{wt}\%M)}{[\text{wt}\%M]}$$

where (wt% M) and [wt% M] represent the mass fraction of M in the slag (s) and the metal (m), respectively. This distribution ratio is an indication where Sn prefers being, i.e. in the slag or the metal. The compositional measurements of the slag phase and the copper phase, and the distribution ratios, are shown in Table 3. The first two measurements have a similar Cu₂O content and the L_{Sn} decreases

Table 2 Experimentally determined phase compositions (wt%) in different areas of the different copper droplets in equilibrium with same CaO–CuO_x–FeO_y–SiO₂–SnO_z slag at 1300 °C. The results do not show any large deviations and it indicates that chemical equilibrium is achieved

		Cu	Sn	Total
Area A (10 points)	Average (wt%)	99.3	0.16	99.4
	Standard deviation (wt%)	0.2	0.02	0.2
	Relative standard deviation of average (%)	0.2	15.0	0.2
Area B (10 points)	Average (wt%)	99.6	0.16	99.8
	Standard deviation (wt%)	0.1	0.02	0.2
	Relative standard deviation of average (%)	0.1	11.1	0.2
Area C (10 points)	Average (wt%)	99.2	0.16	99.4
	Standard deviation (wt%)	0.1	0.02	0.2
	Relative standard deviation of average (%)	0.1	13.0	0.2
Area D (20 points)	Average (wt%)	99.3	0.16	99.4
	Standard deviation (wt%)	0.3	0.03	0.3
	Relative standard deviation of average (%)	0.3	18.0	0.3
Area E (12 points)	Average (wt%)	100.1	0.19	100.3
	Standard deviation (wt%)	0.1	0.05	0.1
	Relative standard deviation of average (%)	0.1	26.8	0.1
Area F (14 points)	Average (wt%)	99.6	0.15	99.7
	Standard deviation (wt%)	0.2	0.03	0.2
	Relative standard deviation of average (%)	0.2	18.7	0.2

Table 3 Normalized measured compositions (wt%) of CaO–CuO_x–FeO_y–SiO₂–SnO_z slag in equilibrium with copper metal at 1300 °C. L_{Sn} (wt%)/(wt%) is the distribution ratio for that system

		Slag				Metal			
		SiO ₂	“Cu ₂ O”	“Fe ₂ O ₃ ”	“SnO ₂ ”	CaO	Cu	Sn	L _{Sn}
1	Average (wt%)	32.4	20.4	42.8	1.6	2.9	99.9	0.09	14.1
	Standard deviation (wt%)	1.2	2.3	1.9	0.1	0.3	0.4	0.04	–
	Rel. standard deviation of average (%)	4	11	4	9	9	0.4	48	–
2	Average	35.7	20.6	38.0	1.55	4.2	99.8	0.16	7.4
	Standard deviation	0.6	0.8	0.6	0.04	0.1	0.4	0.03	–
	Rel. standard deviation of average (%)	2	4	2	3	2	0.4	20	–
3	Average (wt%)	42.8	13.3	32.2	1.85	9.8	99.6	0.40	3.6
	Standard deviation (wt%)	0.3	0.2	0.3	0.03	0.1	1.1	0.06	–
	Rel. standard deviation of average (%)	1	2	1	2	1	1.1	15	–

significantly with increasing the CaO from 2.9–4.2% CaO. The third measurement has a lower Cu_2O concentration, a higher CaO content and a lower distribution coefficient than the other two measurements. The low Cu_2O content, in the sample, indicates that a lower amount of oxygen was present in the system than for the other two samples. Thus, less oxygen is present to oxidize Sn to SnO_2 . Therefore, the decrease of L_{Sn} could be due to the decreased Cu_2O content or due to the increased CaO content, or due to both.

Conclusion

More and more high purity copper scraps are becoming available and these scraps are typically rich in impurities like Sn. The fire refining furnaces are used to treat these scraps and use $\text{Cu}_x\text{O-FeO}_x\text{-SiO}_2$ slags with common additions of CaO. The distribution ratios for Sn have not been determined for these conditions, i.e. higher Cu_2O concentrations in slag than for copper converting conditions. In this paper, the methodology of Sn distribution and the measurement of slag and copper droplets were discussed. The distribution ratio for Sn between copper metal and slag was determined as a function of CaO content in a tridymite saturated slag. At 20.4% Cu_2O and 2.9% CaO, the distribution ratio of Sn was 14.1, whereas at 20.6% Cu_2O and 4.2% CaO, the ratio decreased to 7.4. This decrease indicates that the distribution of Sn is highly dependent on the CaO content in tridymite saturated slag at constant Cu_2O content.

References

1. European Copper Institute (2016) Copper recycling. <http://copperalliance.eu/about-copper/recycling>. Accessed 13 Nov 2017
2. Hidayat T, Henao HM, Hayes PC, Jak E (2012) Phase equilibria studies of Cu–O–Si systems in equilibrium with air and metallic copper and Cu–Me–O–Si systems (Me = Ca, Mg, Al, and Fe) in equilibrium with metallic copper. *Metall Mater Trans B* 43(6):1290–1299
3. Hidayat T, Henao HM, Hayes PC, Jak E (2012) Phase equilibria studies of the Cu–Fe–O–Si system in equilibrium with air and with metallic copper. *Metall Mater Trans B* 43(5):1034–1045
4. Shuva M, Rhamdhani M, Brooks G, Masood S, Reuter M (2016) Thermodynamics data of valuable elements relevant to e-waste processing through primary and secondary copper production: a review. *J Clean Prod* 131:795–809
5. Anindya A (2012) Minor elements distribution during the smelting of WEEE with copper scrap. RMIT University, Australia
6. Yazawa A (1981) Extractive metallurgical chemistry with special reference to copper smelting. In: 28th congress of IUPAC, Vancouver
7. Nagamori M, Mackey PJ (1977) Distribution equilibria of Sn, Se and Te between $\text{FeO-Fe}_2\text{O}_3\text{-SiO}_2\text{-Al}_2\text{O}_3\text{-CuO}_{0.5}$ slag and metallic copper. *Metall Trans B* 8(B):39–46
8. Ilyushechkin A, Hayes P, Jak E (2004) Liquidus temperatures in calcium ferrite slags in equilibrium with molten copper. *Metall Mater Trans B* 35(2):203–215

9. Crivits T, Hayes PC, Jak E (2015) Influence of MgO on the phase equilibria in the $\text{CuO}_x\text{-FeO}_y\text{-MgO-SiO}_2$ system in equilibrium with copper alloy-Part I: methodology and liquidus in the tridymite primary phase field. *Int J Mater Res* 106(5):454–463
10. Fallah-Mehrjardi A, Hidayat T, Hayes P, Jak E (2017) Experimental investigation of gas/slag/mate/tridymite equilibria in the Cu–Fe–O–S–Si system in controlled atmospheres: development of technique. *Metall Mater Trans B* 48(6):3002–3016
11. Batanova V, Soboloev A, Magnin V (2017) Trace element analysis in EPMA: current state and perspectives. In: EMAS, Konstanz
12. Reed SJ (2000) Quantitative trace analysis by wavelength-dispersive EPMA. *Microchim Acta* 132(2):145–151